Optical Flow Field Measurements of The Coolant In A Grinding Machine

Björn Espenhahn (b.espenhahn@bimaq.de)
University of Bremen: Universitat Bremen https://orcid.org/0000-0002-4039-2147
Lukas Schumski
University of Bremen
Christoph Vanselow
University of Bremen
Dirk Stöbener
University of Bremen
Daniel Meyer
University of Bremen
Andreas Fischer
University of Bremen

Research Article

Keywords: grinding, liquid jet, PIV, shadowgraphy, in situ

Posted Date: June 18th, 2021

DOI: https://doi.org/10.21203/rs.3.rs-588246/v1

The International Journal of Advanced Manufacturing Technology manuscript No.
(will be inserted by the editor)

Optical flow field measurements of the coolant in a grinding machine

Björn Espenhahn · Lukas Schumski · Christoph Vanselow · Dirk Stöbener · Daniel Meyer · Andreas Fischer

Received: date / Accepted: date

Abstract Since the cooling mechanism of industrial grinding is not yet fully understood, a measurement of the coolant liquid flow field near the grinding wheel is desired. However, the curved surfaces of the liquid phase result in unpredictable light deflections and reflections, which impedes optical flow measurements. In order to obtain qualitative and quantitative information regarding the flow velocity field of the coolant liquid, shadowgraphy in combination with a pattern correlation technique as well as particle image velocimetry are applied in a grinding machine and studied with respect to their measurement capabilities. Particle image velocimetry enables flow measurements inside the laminar coolant jet, whereby the shadowgraph imaging velocimetry complements these measurements and is in particular suitable for spray-like flow regimes. As a result, optical flow field measurements of the coolant flow in a grinding machine are shown to be feasible, which is required to understand the flow mechanisms that affect the grinding cooling process.

Keywords grinding · liquid jet · PIV · shadowgraphy · in situ

B. Espenhahn · C. Vanselow · D. Stöbener · A. Fischer
University of Bremen, Bremen Institute for Metrology, Automation and Quality Science (BIMAQ), Linzer Str. 13, 28359 Bremen, Germany,
E-mail: B.Espenhahn@BIMAQ.de

L. Schumski · D. Meyer
Leibniz-Institut für Werkstofforientierte Technologien – IWT, Badgasteiner Straße 3, 28359 Bremen, Germany

D. Stöbener · D. Meyer · A. Fischer
University of Bremen, MAPEX Center for Materials and Processes, Postbox 330440, 28359 Bremen, Germany

1 Introduction

1.1 Motivation

Grinding is an essential manufacturing process to produce metallic components. In this process a liquid jet is used for lubrication and cooling of the workpieces to prevent grinding burn [7]. In-depth knowledge of the coolant flow is essential for understanding the heat transfer associated with the grinding process [15]. Several experiments and simulations to characterize the cooling performance for different inflow conditions like various nozzle shapes, inflow angles and volume flows were carried out, whereby only an indirect optimization of the coolant jet flow was performed so far [2,1,11,3,25]. Nevertheless, a flow field measurement of the coolant flow in a grinding machine has not been performed so far. In order to understand the underlying flow mechanisms responsible for an efficient cooling of the grinding process, in-process flow field measurements of the coolant liquid flow velocity are needed [19].

The jet-based cooling of the workpiece and the rotating grinding wheel represent a highly dynamic process and lead to a complex flow. In order to investigate the measurability of the approaching coolant jet, its interaction with the grinding wheel, and its adhesion to the tool, the present study is conducted on a rotating grinding wheel without workpiece.

1.2 State of the art

Qualitative flow investigations in a grinding machine have already been conducted. Geilert et al. [21] used shadowgraphy to visualize the coolant inflow for different nozzles and volume flows. The visualization with

shadowgraphy is based on the influence of light refraction by the observed object (e.g. coolant jet) on a homogeneous background illumination. The difference in the refractive index number of air and coolant generally leads to a deflection of light at their interface. Inhomogeneities in the surface of the coolant become visible, as the evenly distributed illuminating light gets deflected differently [8,9]. The resulting camera image of the illuminated flow is called a shadowgram. With shadowgraphy it is possible to evaluate the free jet shape of the coolant supply [17]. A shadowgram of the coolant supply flow from the nozzle to the interaction with the rotating grinding wheel is shown in Fig.1. However, a quantitative velocity measurement of the coolant flow behavior is required to gain insights regarding the decisive factors for the efficient supply of the contact zone in grinding.

A velocity field measurement based on visualized turbulent structures in air flows was reported by Jonassen et al. [6]. The motion of turbulent structures is evaluated similar to the correlation of seeding particles in particle image velocimetry (PIV). For this measurement approach, the term shadowgram imaging velocimetry (SIV) is used here, which means tracking characteristic flow structures that are visualized with the shadowgram imaging. Note that the 3d-illuminated observation is mapped on a 2d image. Thus, flow structures from different depths are not distinguishable and an averaging effect along the line of sight results.

The shadowgram of the coolant flow in Fig. 1 shows characteristic structures, so that a quantitative velocity measurement of the coolant flow field beyond a qualitative flow visualization seems feasible in principle. In the area after the interaction with the grinding wheel, the coolant is in the form of droplets, which can be detected in the shadowgram with a high contrast and thus are traceable. However, the visualized free jet before the interaction with the grinding wheel has characteristic structures only on the jet surface. Here, it has to be examined, if the visualization is sufficient for a quantitative velocity measurement of the coolant flow. Furthermore, it has to be checked if the correlation of the shadowgrams reflects the actual coolant flow velocity.

Although Doppler methods seem to be more robust against light refractions [23], PIV is preferred here for velocity reference measurements due to its less specific laser requirements. With PIV, a 2d velocity field is obtained by seeding the fluid with tracer particles and observing their motion with one camera. The measurement plane is defined by the light sheet illumination. A double-pulse laser is applied to illuminate particles in the measurement plane with a given time interval enabling to determine the change of the particle position. The density and size of the seeding is adjusted to the flow properties, so that the particles follow the flow with a negligible slip [16]. For the flow field evaluation, two consecutive images of the pulsed illuminations are captured and divided in rectangular interrogation areas. The cross-correlation of each interrogation area from both images results in a displacement vector that corresponds to the local in-plane flow velocity [16].

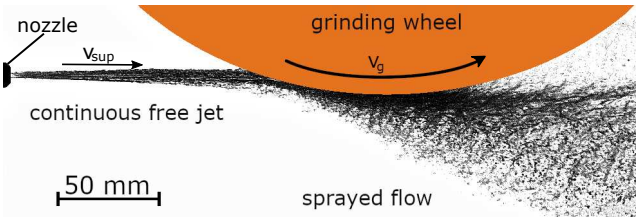

Figure 1: Picture of the coolant flow hitting a rotating grinding wheel without workpiece. The flow is present as a continuous liquid free jet until it is interacting with the grinding wheel, where it gets sprayed.

The impact of light deflection on the PIV measurement technique in two-phase flows depends on the surface geometry of the phase transition. For stationary liquid-air phase transitions, the systematic measurement error can be corrected by ray-tracing and mapping algorithms [13,26]. Consequently, a general measurability with PIV in laminar two-phase flows can be assumed. However, the jet flow in the grinding machine typically has a randomly fluctuating liquid-air phase due to the inflow conditions with velocities up to 60 m/s. This leads to an increase of disturbances in the illumination and observation light path, resulting in an increased measurement uncertainty [22].

For PIV measurements in fluctuating refractive index fields in air, the systematic measurement error has been determined and partially corrected [4,5]. Approaches for measuring and correcting the measurement errors of randomly fluctuating surfaces of the liquid-air phase transition have been proposed, but these are either too slow [18] or only feasible for changes in the scale of micrometer [20]. Indeed, PIV measurements of the coolant flow in a grinding machine have not yet been studied. In particular, the applicability of PIV to measure the free jet flow in a grinding machine needs to be investigated.

1.3 Aim and outline

The article investigates the measurability of the coolant flow velocity in a grinding machine for various volume flows. For the quantification of the velocity field of the free jet, SIV and PIV are applied and studied to serve as complementary measurement techniques. For the coolant

flow that interacted with the grinding wheel, the droplets are used for a flow field measurement with SIV.

The approaches for the velocity field calculation of the coolant flow with SIV and PIV are explained in Section 2. Section 3 gives details of the experimental setup, which is implemented in the grinding machine. The results are shown and discussed in Section 4, where at first the comparison measurements of SIV and PIV of the coolant liquid jet are discussed until measurements of the whole coolant flow including the interaction with the grinding wheel are presented and assessed regarding the flow measurability. The article closes with a summary and an outlook in Section 5.

2 Measurement approach

In order to measure the flow velocity with optical measurement techniques, flow characteristics must be visualized, from which the flow pattern can be derived. As shown in Fig. 1, the flow gets torn up into droplets after interaction with the grinding wheel. There, the appearing droplets are unambiguously allocated in the shadowgram imaging, so that their movement can be observed with high-speed measurements. The 2d velocity field behind the interaction with the grinding wheel can then be calculated with a cross-correlation of consecutive images [12], resulting in a SIV measurement.

The coolant projected from the nozzle onto the grinding wheel is a continuous liquid free jet and for usual volume flows of a grinding process, the flow of the free jet is turbulent [24]. The turbulences within the flow lead to local changes in the free jet surface. The appearing inhomogeneities on the surface are visualizable with the shadowgraphy as characteristic flow structures. They are used as flow tracers for SIV for a quantitative velocity field calculation. Consequently, only the flow velocity at the surface can be determined with the chosen approach.

In order to realize both SIV measurements in the grinding machine, the measurement arrangement depicted in Fig. 2 is proposed. A diffuse background light source is used to illuminate the fluid and a camera on the opposite side records the resulting shadowgram. Note that no depth information is acquired and a superposition of flow structures from different depths of the fluid cannot be separated and disturb the detectability. In order to evaluate the respective measurement uncertainty, the shape of the free jet must be considered.

The coolant supply flow is generated with a nozzle with a rectangular outlet shape. The resulting geometry for the free jet is shown in Fig. 3. According to the rectangular orifice shape, the liquid free jet is formed as a sheet with a thickness and width in the same scale as the orifice shape. However, the outer edges have a rounded cross-section due to the surface tension, that leads to a tapering.

Two different views of the supply flow are subsequently considered: The top and side view. Measurements of the top view of the supply flow result in observations through a thin volume, for which the surface structures can be assumed to be sufficient for the calculation of the total flow velocity. In addition, no superpositions of the characteristic flow structures from different depths occur. However, in order to observe the flow and its interaction with the grinding wheel, images must be taken from the side of the grinding wheel in z-direction. In this arrangement, the coolant supply flow is observed through its entire width. A superimposed observation of the characteristic flow structures from different depths is expected, which results in possible misallocations and a reduced detectability of the flow structures. Therefore, for the side view it is necessary to determine the impact of the volumetric observation on the measurement. For this purpose, an observation of the liquid jet's top view is performed as well and the measurements are compared with each other.

Finally, it must be checked how the movement of the flow characteristics relates to the flow velocity. To achieve this, the velocity of the free jet is additionally determined in both perspectives using PIV as a reference measurement technique. However, due to the influence of light refraction, the feasibility of PIV measurements must also be confirmed. Difficulties might appear for the illumination and observation of the flow tracer particles and are assumed to increase with the presence of flow structures. In order to ensure the feasibility of PIV for measurements in the coolant free jet, measurements are taken at first for a laminar free jet flow, where no unsteady surface structures occur. Once the feasibility has been proven for a laminar supply flow, measurements will be carried out on a laminar-turbulent transient flow, where faint flow structures are present and flow measurements with SIV are feasible, too. A comparison of the absolute measurement uncertainties for the laminar and laminar-turbulent case will show the influence of the uneven surface, caused by the flow structures, on the PIV measurement.

3 Experimental setup and signal processing

3.1 Grinding machine with optical access

The measurements are conducted in a surface grinding machine of the type Micro-Cut A8 CNC manufactured by the company ELB.

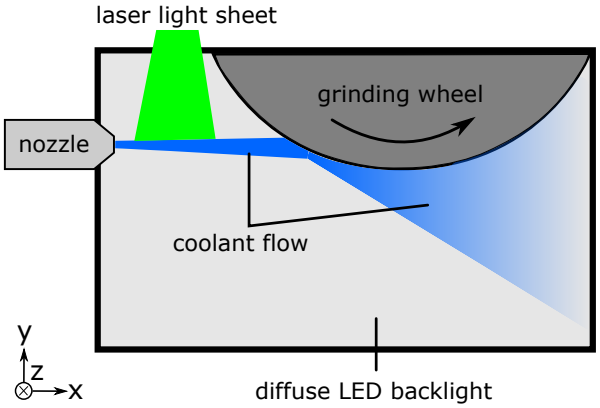

Figure 2: Schematic representation of the flow generation and the velocity measurement in a grinding machine with the laser light sheet illumination for PIV and the diffuse LED backlight illumination for the shadowgram imaging. Recordings are taking with a camera looking in z-direction, centered at the height of the nozzle orifice and moved along the x-axis according to the investigated flow region.

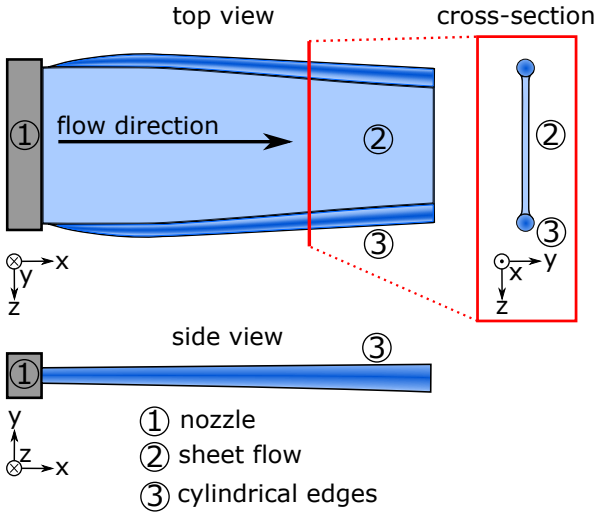

Figure 3: Free jet geometry generated with the rectangular nozzle orifice.

The coolant supply is generated out of a coolant supply nozzle with a specific profile according to Rouse (see Fig. 4) onto the grinding wheel surface. The distance between the nozzle orifice and the point of impact on the grinding wheel is 100 mm. The used coolant is the metal working fluid *CUT MAX 902-10* with a density of 0.82 kg/m^3 and dynamic viscosity of 11 mm^2/s.

For the experimental investigations, the coolant jet is supplied with flow rates of 15 L/min, 25 L/min and 35 L/min. Two different orifice sizes are used with a

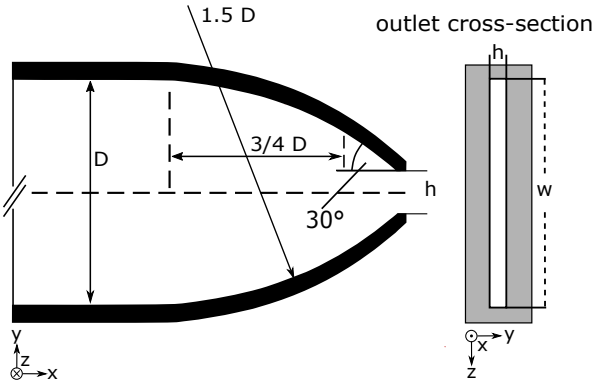

Figure 4: Technical sketch of the Rouse-nozzle, based on Rouse et al. and Webster et al. [10,14].

common width of 21 mm. For investigations on the free jet of the coolant supply, a nozzle with an orifice height $h = 1.6$ mm is used to obtain laminar flow fields. For the coolant flow measurements with the grinding wheel, the nozzle height $h = 0.9$ mm is applied to achieve higher flow velocities for the same volume flows. The grinding wheel has a radius of 200 mm and rotates with a circumferential velocity of 25 m/s. To provide access for the optical components into the grinding chamber during the cooling process, the protective acrylic glass window that closes the grinding chamber is removed and replaced with a transparent foil. Viewing windows are cut into the foil to achieve an undisturbed observation of the volume flows. Work safety is ensured by an external protective housing, which additionally grants laser safety.

For investigating the coolant supply flow in particular, an interaction with the grinding wheel is prevented by moving it out of plane. In order to determine the top view of the coolant free jet flow, the nozzle is rotated by 90° instead of reassembling the optical measurement setup. Finally, the nozzle is placed in its original position and the coolant fluid flow interacting with the rotating wheel is studied.

3.2 Optical setup

The optical setup corresponds with the representation in Fig. 2, which is explained below in detail. A light-emitting diode (LED) panel is installed as a diffuse background illumination on the rear wall within the working area of the grinding machine for flow visualization with shadowgraphy. It provides an illumination of 2400 lm in neutral white (color temperature 4300 K). The distance from the LED panel to the center of the grinding wheel is 250 mm. For the observation, a high-speed camera of the type Pro Y4 from the company

Integrated Design Tools Motion is located at a distance of $z = 60\,\text{mm}$ to the center of the grinding wheel with the camera axis orientated in z-direction. A spatial resolution of 125 µm/px is achieved with the 105 mm F2,8 EX macro objective from the company Sigma and the shadowgrams are recorded with a repetition rate of 13.700 Hz and an exposure time of 50 µs. The exposure time is short enough to capture quasi-stationary images of the flow details.

To obtain also PIV measurements of the coolant supply, polyamid seeding particles with an averaged size of 50 µm and a density of $1.03\,\text{g/cm}^3$ are filled into the coolant tank of the grinding machine. To illuminate the seeded flow, a frequency-doubled pumped Nd:YAG pulsed laser at a wavelength of 532 nm with a maximum energy per pulse of 200 mJ and a pulse length of 10 ns of the type Evergreen from the company Quantel is used. A double pulse repetition rate of 15 Hz is used with a time separation per pulse between 70 µs to 100 µs, which is adjusted according to the flow velocity. The laser light sheet has a width of approximately 50 mm with a sheet thickness of 1 mm. It illuminates 50 mm to 100 mm of the jet length and is placed centered to the width of the nozzle. Note that the laser beam is guided into the grinding machine with a light-guiding arm, that provides the necessary flexibility and protection from contaminating coolant for the optical components. The necessary optics to form a laser light sheet are installed in the grinding machine and protected by a housing to avoid unwanted contamination by coolant droplets. For particle imaging a 5.5 Mpx sCMOS camera of the type Zyla from the company Andor with a 50 mm focal length objective of the type Planar T* 1.4/50 from the company Zeiss is used. The camera is positioned at a distance of $z = 60\,\text{cm}$ to the coolant jet, observing in z-direction and images are taken with a spatial resolution of 80 µm/px. For a reduction of disturbing ambient light, a bandpass filter with central wavelength of 532 nm is used.

3.3 Image enhancement and cross-correlation algorithm

For the velocity field calculation, the captured images for SIV and PIV are visually enhanced and analyzed with the software DynamicStudio, developed by Dantec Dynamics. The image enhancement process uses a spatial median and tophat image filter for eliminating noise in the images. For increasing the detectability of the particles, the Sobel operator is used to highlight horizontal intensity changes and to eliminate visible stationary flow structures from the edges. The velocity field is then calculated with an adaptive PIV algorithm with an overlap of 75 % for an interrogation area size of 32×32 px. Additionally, outliers are detected and removed from the measurements with a range validation. Averaged velocity fields of 1000 single measurements for SIV and 350 for PIV are calculated to minimize the residual impact of measurement outliers. Additionally, the standard deviation of the mean is determined as a measure of the measurement uncertainty.

4 Measurement results

The impact of optical distortions on flow measurements of the coolant jet is discussed in Section 4.1. In Section 4.2 the PIV measurement is shown to be feasible for a laminar coolant jet flow and further used as a reference to determine the flow behavior of the characteristic flow structures of a laminar-turbulent transient flow as used for SIV, which is shown in Section 4.3.

With the measurability of the coolant supply velocity shown, complete flow field measurements in interaction with the grinding wheel are conducted with SIV and the results are shown in Section 4.4.

4.1 Impact of optical distortions on cooling jet flow measurements

To examine the influence of light refraction on both measuring methods for different inflow conditions qualitatively, raw images are captured with PIV and shadowgram imaging for volume flows of 15 L/min, 25 L/min and 35 L/min. The images are displayed in Fig. 5 and compared with each other.

For the lowest volume flow of 15 L/min a laminar free jet without temporally varying structures results. Considering the top view, a smooth center area is visible and light refractions occur only at the cylindrical edges. In the range of 40 mm to 120 mm of the jet length, the scattered light of the seeding particles is visible and in the side view, the originally round particles are observed significantly distorted due to the curved jet surface and appear as ellipses (see red circle). So in both views, the particles can be identified, which allows to calculate their velocities with PIV via cross-correlation algorithms. Since almost no characteristic flow structures can be observed, a SIV velocity measurement is not possible.

At an increased volume flow of 25 L/min, faint turbulences in the form of waves are present on the free jet geometry. These turbulences follow the flow direction and are visible in the shadowgraphy, which principally enables a SIV velocity evaluation.

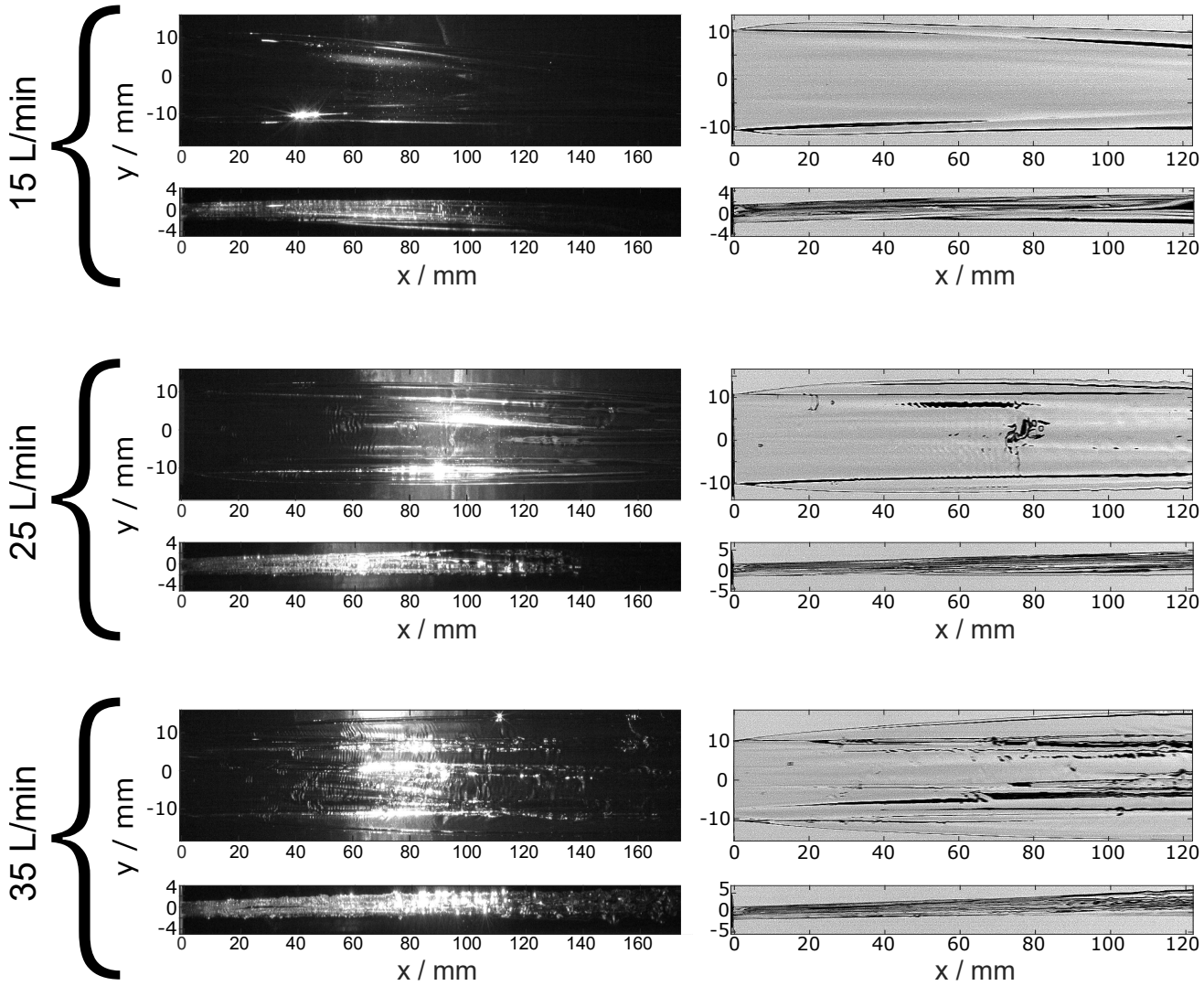

Figure 5: Images of the free jet region for the top- and side view captured with PIV (left) and shadowgram imaging (right). The top- and side view for each volume flow is displayed as a pair.

Due to the turbulences, further light refractions occur in the illumination with the laser light section for PIV, visible at 90 mm of the jet length. However, the occurring light refraction is not significant and the particles are still observable. An evaluation with PIV seems therefore still possible. The comparison of the velocity measurement with SIV (based on flow structures) and PIV (based on seeding) in Sec. 4.3 will reveal, if the characteristic flow structures reflect the flow velocity.

For the flow rate of 50 L/min the turbulences are more intense and the surface of the liquid contains more pronounced inhomogeneities. Due to the dominant surface inhomogeneities, total reflections occur in parts of the wave structures. The influence of the total reflections is a major obstacle for the PIV measurement technique. If they occur, the laser light does not enter the coolant and no particles are illuminated. In addition, the light intensity of the reflections is many times higher than the scattered light from the particles. Even if particles are observed, a light reflection in the immediate vicinity outshines the scattered light from the particles. As a result, a velocity evaluation based on the motion of the particles is no longer possible, since only the wave structures are visualized. The existing turbulent structures are distinguishable in the shadow graph picture and their size increases with the jet length. As a consequence, only measurements with SIV seem feasible.

4.2 Feasibility of PIV on the laminar coolant flow

PIV velocity field measurements are taken for the top and side view of the laminar coolant supply flow with a flow rate of 15 L/min.

The averaged 2d velocity fields and their corresponding uncertainties for the jet positions from 40 mm to 120 mm for the top and side view are displayed in Fig. 6. The flow directions are shown by their vectors and the background displays the color coded magnitude of the velocity components U in m/s.

The measurement from the top view reveals a homogeneous velocity field along the jet length. In the middle area from −5 mm to 5 mm in the y-direction the velocity is constant along the whole jet length at 5.55 m/s. In contrast, the bottom edge of the flow (y = −5 mm to −10 mm) shows a systematically lower velocity of 5.4 m/s. This difference in the measurement can be caused by the cylindrical edge, which is responsible for possible light deflections. To exclude systematic measurement errors due to light deflection, the following analysis focuses on the homogeneous range from y = −5 mm to 5 mm.

The uncertainties of the measurements increase, when the signal-to-noise ratio decreases due to poor illumination. The area from 60 mm to 100 mm of the jet position is well illuminated and shows an uncertainty of 0.2 m/s. In the poorer illuminated region, the uncertainty increases to 0.6 m/s. Hence, PIV measurements of the laminar coolant supply flow are achieved with uncertainties of approximately 4 % in the well illuminated region despite the difficult measurement conditions regarding accessibility and the influence of light refraction.

Subsequently, the measurements of the top and side views can be compared to identify systematic influences of light refraction. Unlike to the top view, the measurement from the side view shows a linear decreasing velocity from 5.6 m/s to 5.4 m/s with a constant uncertainty of 0.2 m/s. For better illustration of the flow velocity along the jet length, the average along the y-axis is calculated and displayed in Fig. 7 for the top- and side view. The average velocities along the jet length are displayed as a solid line and their standard deviation as the colored background.

The top view shows a constant average velocity of 5.55 m/s without any significant changes along the jet length. In comparison, in the side view at first a small increase from 5.6 m/s to 5.64 m/s is measured, until it decreases almost linearly to 5.4 m/s. The differences in the velocity are attributed to the observation of seeding particles through the curved surface of the cylindrical edges. Due to light deflections, a systematic position deviation between the observed and original position of the tracer particles occurs, which leads to systematic measurement deviations for the position and thus also for the velocity. Although the side view measurements are systematically affected by light refraction, this effect is small enough that measurements of both views are within their confidence intervals for the sheer random deviations. Therefore, a flow field measurement on the laminar coolant supply flow with PIV for top and side view are feasible.

4.3 Verification of SIV

To determine how the movement of the characteristic flow structures relates to the flow velocity, SIV and PIV measurements on the coolant supply flow are compared with each other. For this purpose, the flow rate of 25 L/min is used, which sets the coolant supply flow in a laminar-turbulent state. Minor characteristic flow structures are present, which allow measurements with SIV, and PIV provides plausible measurement results, since the seeding particles are still detectable. Similar to the analysis in Section 4.2, the 2d velocity fields of PIV and SIV for both views are determined.

In Fig. 8 a) the averaged velocity fields of PIV and SIV from top view are shown for jet positions from 20 mm to 120 mm. The velocity fields of both measurements are nearly in agreement and show a homogeneous flow field around 9.5 m/s. It is noticeable that the PIV measurement indicates lower velocities at the lateral edges, which is caused by the refraction of light at the cylindrical geometry. On the other hand, the measurement with SIV in the position of 20 mm to 50 mm and y = 0 mm to −10 mm shows a slightly lower velocity.

In Fig. 8 b), the top view mean velocities and their uncertainties for the area without the cylindrical geometries (y = −5 mm to 5 mm) for PIV and SIV are displayed. The velocities are well matched and have a maximum deviation of 0.1 m/s. A slight increase of the velocity in the range of 20 mm to 80 mm from 9.5 m/s to 9.75 m/s is noticeable, until the velocity remains constant. The increase of the velocity is within the measurement uncertainties caused by random measurement deviations and therefore no statements about a systematic deviation can be made. The uncertainties are largely constant for both measurements with 0.3 m/s for PIV and 0.6 m/s for SIV.

The measurements for the side view of the coolant supply flow are shown in Fig. 8 c). The flow field of the PIV measurement is in the range of 9.8 m/s to 9.5 m/s, whereas the SIV measurement is systematically 0.3 m/s lower with velocities in the range of 9.5 m/s to 9.2 m/s. This difference in the averaged velocity is explainable

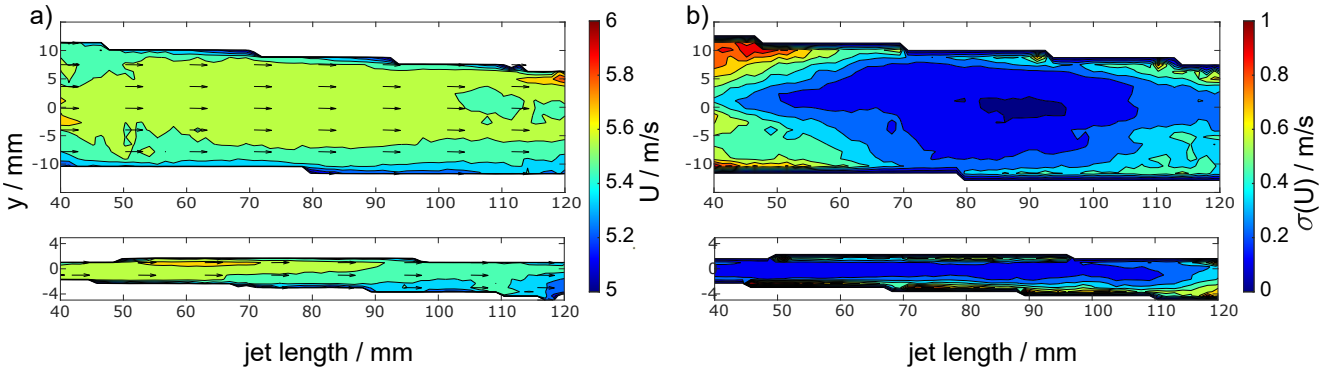

Figure 6: Calculated velocity field for the top- and side view (left) and the corresponding standard deviation (right) for a volume flow of 15 m/s.

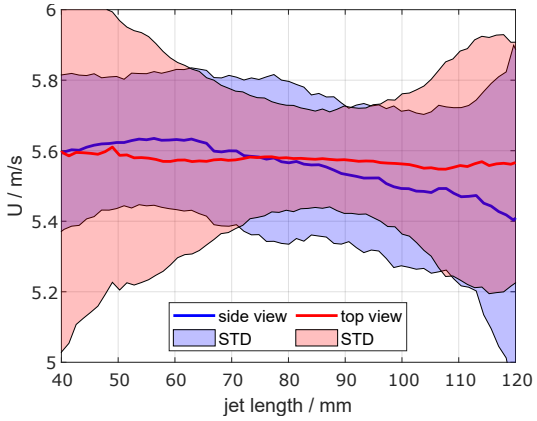

Figure 7: Mean flow velocity for top (red)- and side view (blue) displayed with their standard deviation for a volume flow of 15 m/s.

on the basis of the mean velocities and corresponding uncertainties as displayed in Fig. 8 d). The curves of the velocities are almost identical for both measurements, with a standard uncertainty of 0.3 m/s for PIV and 1.0 m/s for SIV. Due to the higher uncertainty, the PIV measurement is in the confidence interval of SIV. This shows the limitations of the measurement based on the characteristic flow structures. The increased uncertainty due to superposition of characteristic structures from different planes provides a less precise measurement with the SIV, but still ensures velocity measurements from the cooling supply flow with uncertainties around 10.8 % in the side view.

To compare the measurement conditions with respect to the feasibility of PIV and SIV, the globally averaged velocities for the coolant supply flows for the volume flows of 15 L/min and 25 L/min are listed in Tab. 1. The measurements with PIV have an almost constant standard uncertainty of 3.6 %, regardless of the view or the used volume flow. The SIV measurement of the top view has an by 0.3 m/s increased uncertainty of 0.6 m/s (6.1 %). The increased measurement uncertainty of SIV is explainable by deformations of the characteristic flow structures. Each deformation adds a random velocity component on the actual flow velocity and thus leads to an increased standard deviation. For the measurement of the side view, the uncertainty of SIV increases further by additional 0.4 m/s to 1.0 m/s (10.8 %). This is caused by the superposition of the flow characteristics resulting from the observation along the width of the coolant flow. The structures from different depths cannot be distinguished from each other and misallocations of the structures result in outliers which increases the calculated standard uncertainties. This assumption is confirmed by the unchanged measurement uncertainties for PIV, where the observation of particles is reduced to the plane of the laser light sheet. This shows that the PIV measurement yields a more precise flow measurement, however, the SIV offers an adequate alternative.

Although the measurement with SIV is less accurate than PIV, especially for the side view, the velocity fields of the coolant supply flow measured by PIV and SIV are nevertheless consistent within the limits of the measurement uncertainties. This confirms the assumption of the applicability of the characteristic flow structures of the coolant supply flow for a velocity measurement.

4.4 Flow field with rotating grinding wheel

The flow velocity field of a cooling process in a grinding machine without a workpiece is measured for volume flows of 15 L/min, 25 L/min and 35 L/min. With the approach of the SIV, the characteristic flow structures of the coolant supply flow before interaction, as well as the emerging droplets after interaction with the grinding wheel are used for a velocity calculation. As a mea-

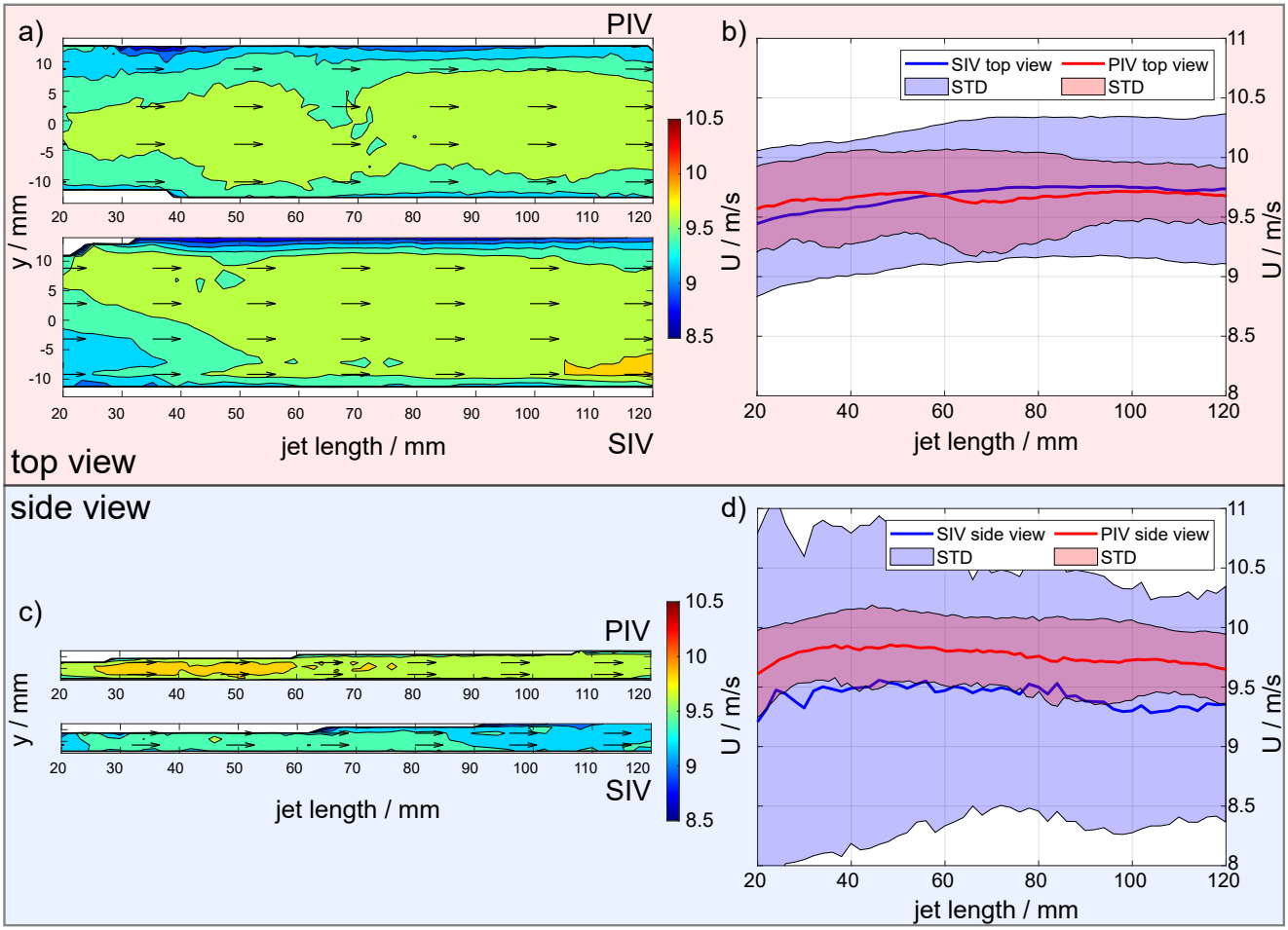

Figure 8: Measured and averaged velocity fields for a volume flow of 25 L/min in top- and side view of the coolant jet with PIV and SIV. a) Averaged 2d velocity field from the top view. b) Mean velocity and uncertainties of the top view along the jet length. c) Averaged 2d velocity field from the side view. d) Mean velocity and uncertainties of the side view along the jet length.

Table 1: Calculated free jet velocities and standard uncertainties for PIV and SIV measurements of the coolant free jet.

Q / L/min	View	PIV	SIV
15	top	(5.56 ± 0.20) m/s	-
	side	(5.54 ± 0.17) m/s	
	rel. error	3.1 %–3.6 %	
25	top	(9.57 ± 0.33) m/s	(9.62 ± 0.59) m/s
	side	(9.63 ± 0.33) m/s	(9.33 ± 1.01) m/s
	rel. error	3.6 %	6.1 %–10.8 %

sure for the coolant supply flow condition, the velocity ratio $R = \frac{v_{\mathrm{sup}}}{v_{\mathrm{g}}}$ of the coolant supply flow v_{sup} to the circumferential velocity of the grinding wheel $v_{\mathrm{g}} = 25\,\mathrm{m/s}$ is used. A range of $R \approx 0.8 - 1.0$ is assumed to be adequate for a sufficient coolant supply condition [19]. To obtain the quantitative coolant supply velocity v_{sup} from the SIV measurements, the flow structures in the homogeneous area of x = 80 mm to 110 mm are used (see Fig. 9 a)). The velocity ratios R range from 0.496 to 1.04 and are listed in Tab. 2 together with the calculated coolant supply flow velocities. A smaller nozzle height of $h = 0.9\,\mathrm{mm}$ is applied to achieve higher flow velocities for the same volume flows.

Table 2: Measured flow velocities of the coolant supply flow and velocity ratio for the used volume flows.

Q / L/min	v_{sup} / m/s	R $= \frac{v_{\mathrm{sup}}}{v_{\mathrm{g}}}$
15	12.4 ± 1.3	0.496 ± 0.052
25	19.1 ± 1.8	0.764 ± 0.072
35	26 ± 2.8	1.04 ± 0.11

To depict the results, the calculated averaged velocity fields are plotted in Fig. 9 as color coded vectors in the corresponding shadowgram image. To present the

capabilities of SIV regarding the flow field of a grinding process, the determined flow fields are discussed qualitatively and quantitatively in relation to the coolant supply conditions.

With the impact of the coolant on the grinding wheel at x = 120 mm, the flow splits in two parts. One part of the flow adheres to the surface of the grinding wheel and the other gets deflected. The adherent flow gets accelerated to the circumferential velocity of the grinding wheel until it loses adherence due to centripetal forces. This results in differences in velocity between the adherent and deflected flows, which can be seen in a sheared flow in the area of x = 180 mm to 280 mm and y = −20 mm to 0 mm. An increase in the velocity field in this area is observed for the volume flows of 15 L/min ($R = 0.50$) and 25 L/min ($R = 0.76$).

For the volume flow of 35 L/min ($R = 1.04$), the jet velocity is higher than the circumferential velocity of the grinding wheel, which leads to a different characteristic in the visualized flow field and its velocity field. In the region of x = 180 mm to 280 mm and y = −30 mm to −10 mm, a droplet structure is observable, which appears to be the deflected supply flow. Despite the interaction with the grinding wheel, the liquid is largely coherent and moves with a velocity above the circumferential velocity. The investigations indicate that for a velocity ratio of $R = 1.04 > 1$ most of the coolant gets deflected instead of entrained into the grinding process. This observation matches the fact that above a certain flow rate, no further increase in heat dissipation can be achieved [19]. A fluid dynamical change which might induce this phenomenon is elaborated by the qualitative visualization of the flow, as well as the calculated quantitative flow field.

A limitation in the evaluation is given in the area of the first interaction of the coolant supply close to the grinding wheel. The shape of the flow has changed in comparison to the free jet, but is not yet torn apart into droplets. The flow is opaque and no flow structures are detectable. The two present flows in this area (deflected and entrained) are subsequently torn into droplets. The further the flow is apart from the grinding wheel, the more has the flow separated into droplets. The detectability of the droplets and thus also the evaluability of the flow field increases steadily with the distance to the grinding wheel. Therefore, the obtained velocities before and after the interaction are plausible and flow structures are assignable to the flow fields and fluid dynamic phenomena like a shear layer are obtainable, whereas the flow velocity close to the grinding wheel is difficult to obtain with the shadowgram imaging.

5 Conclusion and outlook

For the first time optical measurements of the coolant flow in the grinding process without workpiece are conducted in a grinding machine. The flow field measurement is based on characteristic flow structures, which are visualized with shadowgraphy and used as flow tracers for SIV. For the coolant supply flow, the flow behavior of emerging turbulent flow structures is used, which is proven suitable for SIV measurements by referencing with PIV measurements. Once the coolant gets in contact with the grinding wheel, occurring droplets serve as flow tracers for a velocity calculation with SIV.

The measurements on the *coolant supply flow* revealed systematic measurement deviations, which need further examinations to allow an appropriately resolved measurement of the coolant supply flow behavior along the jet length. Measurement deviations are most likely contributed by the light deflection at the liquid-air phase transition. According to the curved surface at the origin of the free jet, a skewed observation is made, which systematically alters the velocity. Random measurement deviations are statistically determined from the measurement series. For PIV, maximum random measurement uncertainties of 4 % result, independent of the measurement arrangement. In comparison, the measurements for SIV can be stated with uncertainties of 6 % for top view and 11 % for side view. Especially in the side view, the superposition in combination with shape shifting of the flow structures leads to a significantly increased uncertainty. Nevertheless, the obtained measurement results provide a first impression of the coolant flow especially of the averaged velocity, which is one of the most significant parameters of the cooling process.

The measured velocity flow fields after an *interaction on the grinding wheel* are verified with a plausibility check of the qualitative visualized flow fields. The occurring velocity changes due to the interaction at the grinding wheel agree with the absolute velocity values as well as its direction. Solely the flow in the direct contact with the grinding wheel is not measurable due to structures that cannot be resolved. Here, further investigations regarding the measurability of the flow in relation to the illumination conditions are recommended.

With the SIV measurements before and with contact with the grinding wheel, the interactions between the flow velocity of the coolant supply and the circumferential velocity of the grinding wheel are examinable. A quantifiable effect of the variations in velocity between inflow and circumferential velocity has already been seen, however research is still pending on, e.g., different angles of incidence, nozzle geometries as well as grinding wheel surfaces.

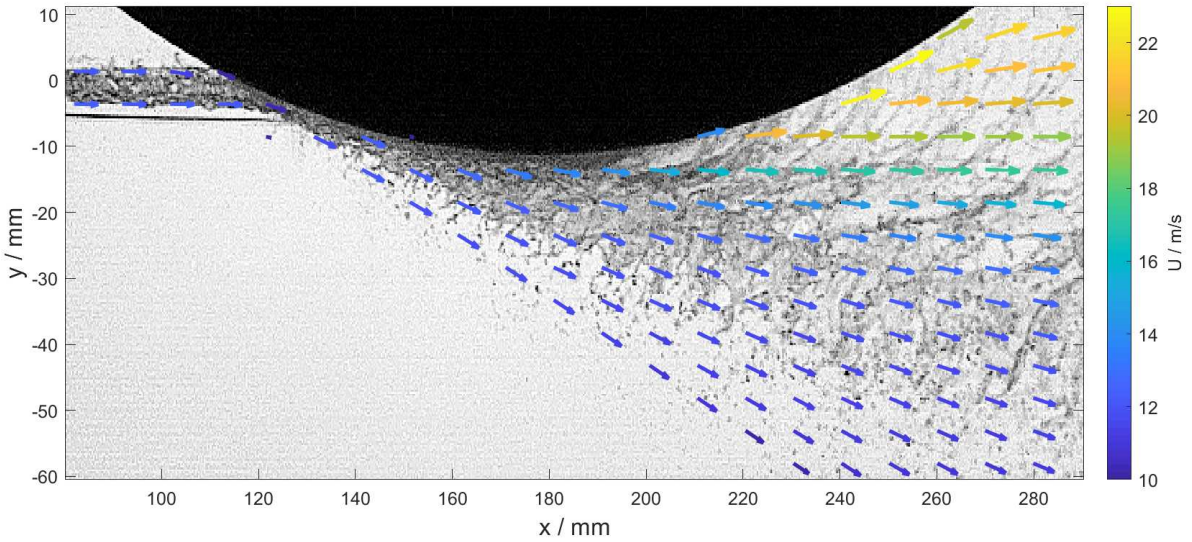

a) $Q = 15\,\mathrm{L/min}$, $v_{\mathrm{sup}} = (12.0 \pm 1.3)\,\mathrm{m/s}$

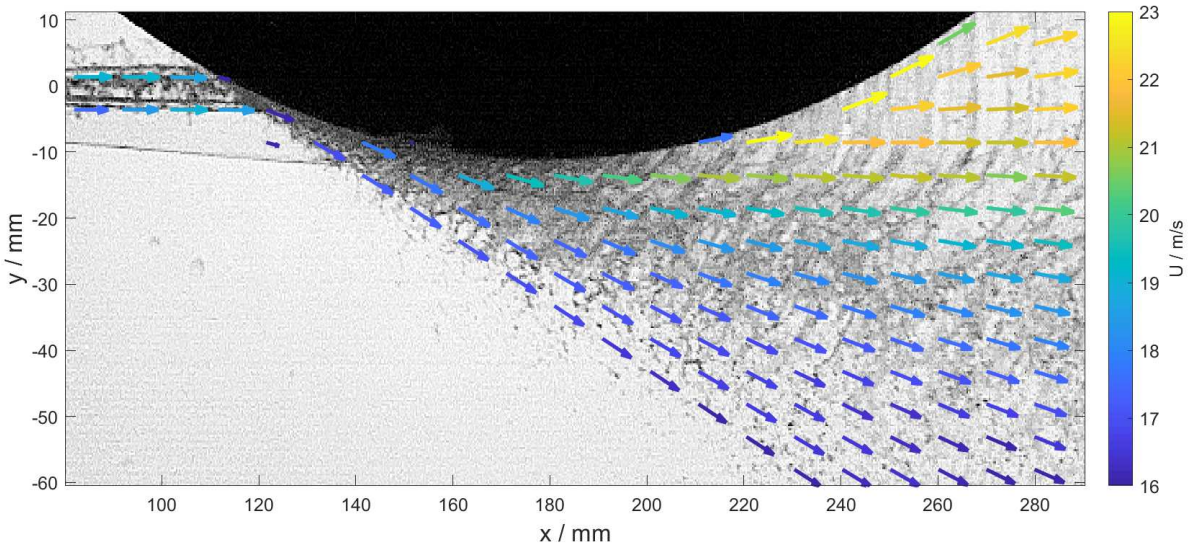

b) $Q = 25\,\mathrm{L/min}$, $v_{\mathrm{sup}} = (19.0 \pm 1.8)\,\mathrm{m/s}$

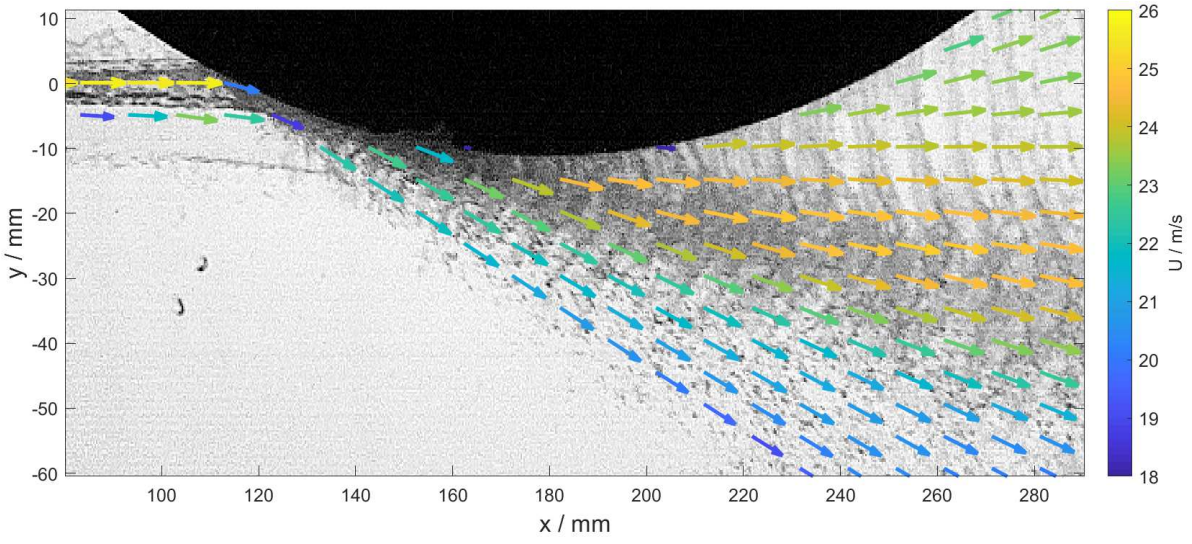

c) $Q = 35\,\mathrm{L/min}$, $v_{\mathrm{sup}} = (26.0 \pm 2.8)\,\mathrm{m/s}$

Figure 9: Snapshot of the shadowgram imaging expanded with the averaged velocity field for the coolant flow that is interacting with the grinding wheel.

The results obtained show the feasibility of quantitative SIV flow measurements for the supply flow of the coolant, as well as for the flow after the grinding wheel interaction. This is the key to the future understanding of the connection between the cooling properties of fluid dynamics, and thus to the further development of optimized cooling in grinding.

Compliance with Ethical Standard

Author Contribution Conceptualization: B.E., C.V., D.S. and A.F.; investigation: B.E. and L.S., supervision: D.M. and A.F.; visualization: B.E., writing-original draft: B.E.; writing-review & editing: C.V., D.S., D.M. and A.F. All authors have read and agreed to the published manuscript.

Funding Funded by the Deutsche Forschungsgemeinschaft (DFG, German Research Foundation) – 415003387

Ethical Approval Not applicable.

Institutional Review Board Statement Not applicable.

Informed Consent Statement Not applicable.

Data Availability Statement Data will be made available on request.

Conflict of Interest The authors declare that they have no conflict of interest.

References

1. C. Heinzel, B. Kirsch, D. Meyer, J. Webster: Interactions of grinding tool and supplied fluid. CIRP Annals **69**(2), 624–645 (2020). DOI 10.1016/j.cirp.2020.05.001
2. C. Heinzel, D. Meyer, B. Kolkwitz, J. Eckebrecht: Advanced approach for a demand-oriented fluid supply in grinding. CIRP Annals **64**(1), 333–336 (2015). DOI 10.1016/j.cirp.2015.04.009
3. C. Li, Q. Zhang, S. Wang, D. Jia, D. Zhang, Y. Zhang, X. Zhang: Useful fluid flow and flow rate in grinding: an experimental verification. The International Journal of Advanced Manufacturing Technology **81**(5-8), 785–794 (2015). DOI 10.1007/s00170-015-7230-z
4. C. Vanselow, A. Fischer: Influence of inhomogeneous refractive index fields on particle image velocimetry. Optics and Lasers in Engineering **107**, 221–230 (2018). DOI 10.1016/j.optlaseng.2018.03.020
5. C. Vanselow, D. Stöbener, J. Kiefer, A. Fischer: Particle image velocimetry in refractive index fields of combustion flows. Experiments in Fluids **60**(10) (2019). DOI 10.1007/s00348-019-2795-1
6. D. R. Jonassen, G. S. Settles, M. D. Tronosky: Schlieren "piv" for turbulent flows. Optics and Lasers in Engineering **44**(3-4), 190–207 (2006). DOI 10.1016/j.optlaseng.2005.04.004
7. E. Brinksmeier, D. Meyer, A.G. Huesmann-Cordes, C. Herrmann: Metalworking fluids—mechanisms and performance. CIRP Annals **64**(2), 605–628 (2015). DOI 10.1016/j.cirp.2015.05.003
8. G. S. Settles: Schlieren and Shadowgraph Techniques. Springer Berlin Heidelberg (2001). DOI 10.1007/978-3-642-56640-0
9. G. S. Settles, M. J. Hargather: A review of recent developments in schlieren and shadowgraph techniques. Measurement Science and Technology **28**(4), 042001 (2017). DOI 10.1088/1361-6501/aa5748
10. H. Rouse, M. Asle, J. W. Howe, D. E. Metzler: Experimental investigation of fire monitors and nozzles. 117th ASCE Transactions (1952)
11. H. Sasahara, T. Kikuma, R. Koyasu, Y. Yao: Surface grinding of carbon fiber reinforced plastic (cfrp) with an internal coolant supplied through grinding wheel. Precision Engineering **38**(4), 775–782 (2014). DOI 10.1016/j.precisioneng.2014.04.005
12. J. Menser, F. Schneider, T. Dreier, S. A. Kaiser: Multipulse shadowgraphic rgb illumination and detection for flow tracking. Experiments in Fluids **59**(6) (2018). DOI 10.1007/s00348-018-2541-0
13. J. R. Castrejón-Pita, S. D. Hoath, I. M. Hutchings: Velocity profiles in a cylindrical liquid jet by reconstructed velocimetry. Journal of Fluids Engineering **134**(1) (2012). DOI 10.1115/1.4005669
14. J.A. Webster, C. Cui, R.B. Mindek, R. Lindsay: Grinding fluid application system design. CIRP Annals **44**(1), 333–338 (1995). DOI 10.1016/S0007-8506(07)62337-3
15. M. Gradeck, A. Kouachi, J.L. Borean, P. Gardin, M. Lebouché: Heat transfer from a hot moving cylinder impinged by a planar subcooled water jet. International Journal of Heat and Mass Transfer (2011). DOI 10.1016/j.ijheatmasstransfer.2011.07.038
16. M. Raffel, C. E. Willert, F. Scarano, C. J. Kähler, S. T. Wereley, J. Kompenhans: Particle Image Velocimetry A Practical Guide. Springer International Publishing (2018). DOI 10.1007/978-3-319-68852-7
17. M. Tadjfar, A. Jaberi: Effects of aspect ratio on the flow development of rectangular liquid jets issued into stagnant air. International Journal of Multiphase Flow **115**, 144–157 (2019). DOI 10.1016/j.ijmultiphaseflow.2019.03.011
18. M. Teich, J. Grottke, H. Radner, L. Büttner, J. W. Czarske: Adaptive particle image velocimetry based on sharpness metrics. Journal of the European Optical Society-Rapid Publications **14**(1) (2018). DOI 10.1186/s41476-018-0073-0
19. M.N. Morgan, A.R. Jackson, H. Wu, V. Baines-Jones, A. Batako, W.B. Rowe: Optimisation of fluid application in grinding. CIRP Annals **57**(1), 363–366 (2008). DOI 10.1016/j.cirp.2008.03.090
20. N. Koukourakis, B. Fregin, J. König, L. Büttner, J. W. Czarske: Wavefront shaping for imaging-based flow velocity measurements through distortions using a fresnel guide star. Optics Express **24**(19), 22074 (2016). DOI 10.1364/OE.24.022074
21. P. Geilert, C. Heinzel, A. Wagner: Grinding fluid jet characteristics and their effect on a gear profile grinding process. Inventions **2**(4), 27 (2017). DOI 10.3390/inventions2040027
22. R. Schlüßler, J. Czarske, A. Fischer: Uncertainty of flow velocity measurements due to refractive index fluctuations. Optics and Lasers in Engineering **54**(1), 93–104 (2014). DOI 10.1016/j.optlaseng.2013.10.011
23. R. Schlüßler, J. Gürtler, J. Czarske, A. Fischer: Planar near-nozzle velocity measurements during a single high-pressure fuel injection. Experiments in Fluids **56**(9) (2015). DOI 10.1007/s00348-015-2044-1

24. S. P. Lin, R. D. Reitz: Drop and spray formation from a liquid jet. Annual Review of Fluid Mechanics **30**(1), 85–105 (1998). DOI 10.1146/annurev.fluid.30.1.85
25. W. Stachurski, J. Sawicki, K. Krupanek, K. Nadolny: Numerical analysis of coolant flow in the grinding zone. The International Journal of Advanced Manufacturing Technology **104**(5-8), 1999–2012 (2019). DOI 10.1007/s00170-019-03966-x
26. Y. Wu, Y. Liu, S. Shao, J. Hong: On the internal flow of a ventilated supercavity. Journal of Fluid Mechanics **862**, 1135–1165 (2019). DOI 10.1017/jfm.2018.1006